Axial ratio improvement of an Archimedean spiral antenna over a radial AMC reflector

M. Grelier[1,2*], C. Djoma[1,2], X. Begaud[1], A. C. Lepage[1], M. Jousset[2] and S. Mallégol[2]

[1]Institut Telecom, Telecom ParisTech - LTCI CNRS UMR 5141,
46 rue Barrault 75634 Paris Cedex 13, France
[2]Thales Systèmes Aéroportés, 10 avenue de la 1ère DFL 29238 Brest Cedex 3, France
*Corresponding author: grelier@ieee.org

Abstract

This paper presents a method to improve the circular polarization of an Archimedean spiral antenna placed over a radial Artificial Magnetic Conductor (AMC). Results have been compared with the same radiating element over a more classical AMC reflector. A prototype of an Archimedean two-wire spiral antenna has been built to operate from 0.5GHz to 6GHz. Measurement results with this radial AMC give a relative bandwidth of 79%, in which the broadside RHCP gain is improved. In this bandwidth the axial ratio is less than 2dB whereas it is higher than 3dB with a classical cartesian shape of AMC reflector.

1. Introduction

The needs of the current wireless applications, both civilian and military, require antennas that are at the same time, low cost, low thickness and broadband. Planar spiral antennas are widely used to fulfill the aforementioned specifications. An Archimedean spiral antenna radiates a circularly polarized bi-directional beam. In most applications, this bi-directional beam must be transformed into a unidirectional one. A classical solution consists in backing a cavity filled by an electromagnetic absorber behind the radiating element. However, the antenna is bulky and loses one half of the radiated power.

Another approach consists in taking advantage of the backward radiated electric field by reflecting it in-phase with the forward radiated electric field thanks to an Artificial Magnetic Conductor (AMC) [1]. In [2], a reflector based on AMC called Quasi Artificial Magnetic Conductor (QAMC) has been presented. The term "quasi" has been chosen because the QAMC is composed of a few elementary cells.

In this paper we present the improvement of the cartesian QAMC by a reflector suitable to the geometry and the radiation of the Archimedean spiral antenna. The spiral antenna is presented in section 2. The method to design the QAMC is introduced in section 3. In section 4 the spiral antenna is placed over the two different QAMC and compared in order to validate the new design. Then measurements are presented and discussed.

2. Archimedean spiral antenna

The two-wire Archimedean spiral antenna introduced by Kaiser [3], is widely used in airborne systems due to its wideband intrinsic characteristics. This kind of antenna has active areas which depend of the frequency. Thus, these areas are defined by $D=\lambda/\pi$, where D is the diameter of the area and λ the free space wavelength. The knowledge of these active areas enables to adapt the geometry of the reflector to these areas.

The inner diameter and the outer diameter of the prototype of the Archimedean two-wire spiral antenna are respectively D_{in}=6.3mm and D_{out}=300mm which define, respectively, the highest and the lowest operating frequencies f_{high}=15GHz and f_{low}=0.3GHz. Nevertheless, we are going to present results from 0.5GHz to 6GHz, because it is the required bandwidth for the targeted application. The width of the spiral arms is w_{arm}=1.25mm, the spiral arms are separated with a distance equal to the arm width to produce a self-complementary structure and thus maintain broadband characteristics [4].

The antenna is printed on a dielectric substrate Duroid RT5880, the thickness is h_{sub}=1.575mm, the relative dielectric permittivity is ε_r=2.2 and the dissipation factor is tanδ=0.0009 (@10GHz).

3. AMC Reflector

3.1. Cartesian QAMC reflector

The reflection phase is defined as the phase of the reflected electric field at the reflecting surface.

It is normalized to the phase of the incident electric field at the reflecting surface. The reflection phase method is used to identify the frequency band in which the AMC behavior occurs [5]. In the case which the AMC is an infinite periodic structure, the phase diagram can be obtained by applying periodic conditions of Floquet on an elementary cell in order to simulate an infinite AMC [6].

The AMC bandwidth depends on their dimensions [7] and has been defined for a reflection phase varying between +/-120° [8]. In this bandwidth the spiral antenna placed over an AMC reflector should have a broadside gain higher than the spiral antenna in free space.

The dimensions of the AMC are w=17.35mm and g=2.65mm, where w is the length of a square patch and g the gap between two patches (cf. Fig. 2a).

The AMC substrate is Arlon CuClad 250 with a thickness h_{amc}=4 x 1.565mm, the relative dielectric permittivity is ε_r=2.5 and the dissipation factor is tanδ=0.0018 (@10GHz).

The cartesian QAMC reflector shown in Fig. 2a is composed of a planar array of only 4x4 elementary cells [2]

and it is placed 4mm under the antenna substrate. The diameter of the QAMC reflector is equal to λ_{1GHz}/π (100.8mm).

3.2. Radial QAMC reflector

The radial QAMC reflector resulting from the transformation of the cartesian one is shown in Fig. 2 The method consists in placing the patches under the targeted active area [9]. The active area at a given frequency can be identified by using the electromagnetic energy density (cf. Fig. 1) defines as follows (1).

$$\rho_{EM} = \frac{1}{2}(\varepsilon_0 E^2 + \mu_0 H^2) \quad (1)$$

Where ε_0 and μ_0 are the permittivity and the permeability in free space, E and H are the magnitude of the electric and magnetic fields.

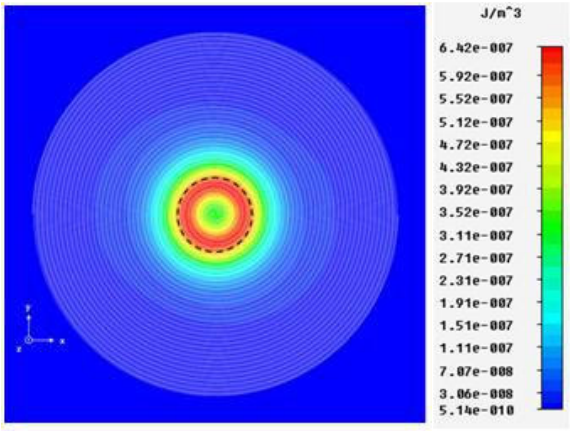

Figure 1: Electromagnetic energy density at 2.5GHz.

The dimensions of the radial patches are the same as for the square patches, i.e. they have a length equal to w and the gap between two patches in the radial or ortho-radial direction is equal to g (cf. Fig. 2b).
The radial QAMC is composed of 2 rows of 12 patches. The distance between the center of the radial QAMC and half the length (w/2) of a patch of the first row (cf. Fig. 2b) is chosen so that the patches operate under this active area at the frequency for which the phase reflection of the AMC is equal to zero. (cf. Fig. 3). This occurs at 2.7GHz and $D_{2.7GHz}$=35.34mm).
The second row is only present to assure the periodicity in the radial direction.

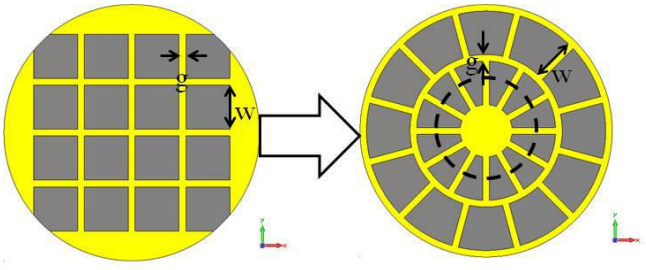

(a) (b)

Figure 2: QAMC top view: (a) Cartesian QAMC, (b) Radial QAMC.

3.3. Results

The Archimedean spiral antenna defined in section 2 has been simulated over the two aforementioned QAMC. Figure 3 presents the broadside realized gain for the co-polarization and the cross-polarization radiated by the antenna and also the phase diagram of the AMC defined in section 3.1. Simulations have been performed with CST Microwave Studio®.

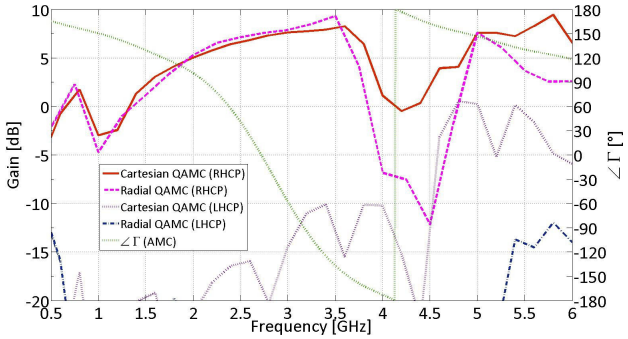

Figure 3: Left scale (simulated gain): Comparison between the two QAMC, Right scale (phase): Reflection phase diagram of the AMC.

According to Fig 3. the reflection phase of the AMC is included between +/-120° from 1.68GHz to 3.36GHz and leads to a relative bandwidth of 66%. Fig. 3 shows that the spiral antenna placed over a cartesian QAMC has a broadside LHCP gain (cross-polarization component) higher than -10dB from 4.5GHz to 6GHz. The spiral antenna placed over a radial QAMC has a broadside LHCP gain less than -10dB from 0.5GHz to 6GHz. The two configurations have a similar broadside RHPC gain (co-polarization component) from 1GHz to 3.5GHz. In order to validate those results, a prototype has been realized.

4. Configurations

We present hereafter the different configurations that have been measured. The configuration named AS_{Ref}, corresponds to the spiral antenna placed above a cavity completely filled with an electromagnetic absorber, with a height h_{abs}=55.26mm (cf. Fig. 4).
This configuration will be used as the reference to evaluate the benefits of the proposed structures.

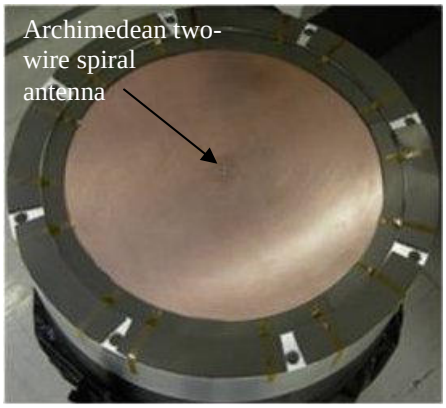

Figure 4: Spiral antenna over the cavity.

The distance between the antenna substrate and the surface of the QAMC reflectors is h_{air}=4mm (cf. Fig. 5).
So the total thickness of the antenna is equal to $h_t=h_{sub}+h_{air}+h_{amc}$=11.835mm i.e. $\lambda_{1.68GHz}/15$. In order to not disturb the behavior of the spiral antenna at low frequency, absorber is put all around the QAMC reflectors (cf. Fig. 5). These two configurations are named $AS_{C\text{-}QAMC}$ and $AS_{R\text{-}QAMC}$ respectively, where $AS_{C\text{-}QAMC}$ refers to the spiral antenna above the cartesian QAMC and $AS_{R\text{-}QAMC}$ to the spiral antenna above the radial QAMC.

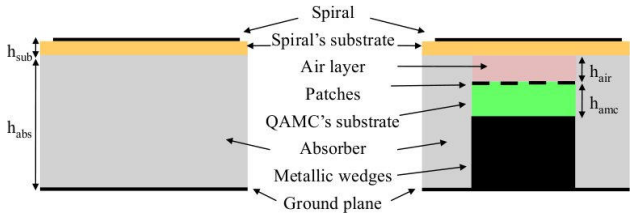

(a) (b)

Figure 5: Configurations: (a) AS_{Ref}, (b) $AS_{C/R\text{-}QAMC}$.

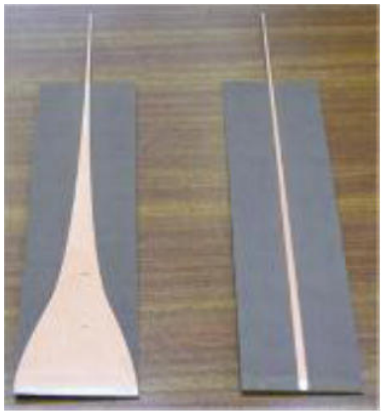

Figure 6: Top and bottom view of the balun.

Figure 7: The whole antenna: Cavity of the antenna assembled with the shielded cavity of the balun.

The antenna is fed at the center of the spiral through a broadband tapered balun (cf. Fig. 6).
It is required to transform the impedance presented by the input balanced line of the spiral equal 160Ω to the unbalanced line of the coaxial connector equal to 50Ω.
The size of the balun is 300mm x 60mm [2], and it is placed in a shielded cavity (cf. Fig. 7).

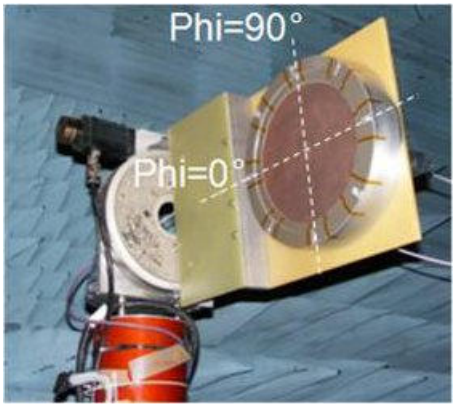

Figure 8: Definition of φ planes.

5. Results and discussion

In this section, measurements of the aforementioned configurations are analyzed.
Fig. 9 shows that the AS_{Ref} has a good impedance matching from 0.5GHz to 6GHz defined for a return loss level less than -10dB.
The $AS_{C\text{-}QAMC}$ has also a good impedance matching from 0.5GHz to 6GHz. The return loss level of the $AS_{Q\text{-}AMC}$ presents a minor increase between 4.7GHz to 4.8GHz.

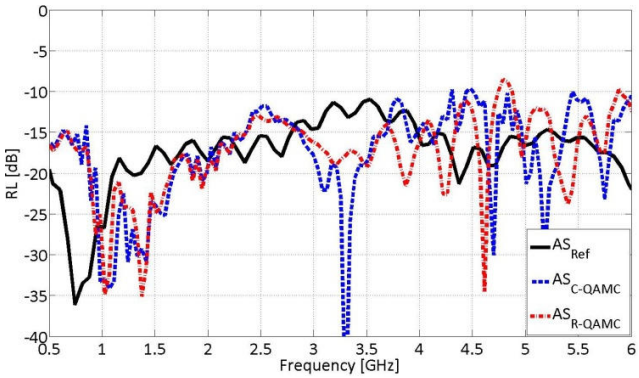

Figure 9: Return loss versus frequency.

Fig. 10 shows the evolution of the broadside RHCP gain (co-polarization component) for the different configurations. We observe the same behavior from 0.5GHz to 3.3GHz for $AS_{C\text{-}QAMC}$ and $AS_{R\text{-}QAMC}$.
For both configurations the broadside RHCP gain is higher than the AS_{Ref} from 1.65GHz to 3.8GHz i.e. a relative bandwidth of 79%. It's interesting to note that this band is greater than the theoretical bandwidth of 66% deduced previously from the phase diagram.

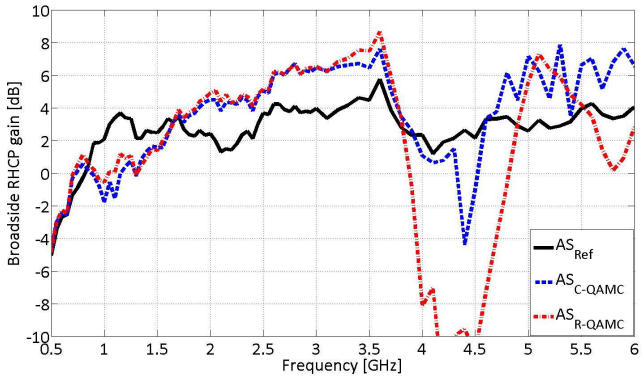

Figure 10: Broadside gain (RHCP) versus frequency.

Fig. 11 presents the broadside LHCP gain (cross-polarization component) for the different configurations. We can see that the broadside LHCP gain of the $AS_{R\text{-}QAMC}$ remains below -10dB from 0.5GHz to 6GHz. Unlike the broadside LHCP gain of the $AS_{C\text{-}QAMC}$ is higher than -10dB for frequencies higher than 3.25GHz.

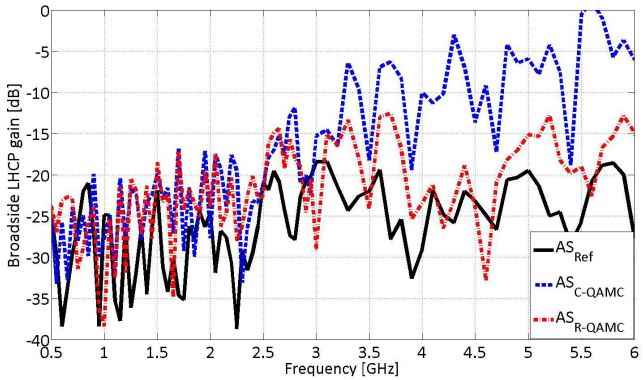

Figure 11: Broadside gain (LHCP) versus frequency.

In order to evaluate the benefits of the radial QAMC the axial ratio (AR), which defines the quality of the circular polarization [10], is presented in figure 12.
The AR level of the AS_{Ref} remains below 3dB from 0.5 GHz to 6GHz i.e. a relative bandwidth of 169%, thanks to the absorber cavity. The AR level of the $AS_{C\text{-}QAMC}$ is less than 3 dB from 0.5GHz to 3.3GHz i.e. a relative bandwidth of 74%. At 4.4GHz broadside RHCP and LCHP gains have the same value and that is why at this frequency the AR level is higher than 10dB. Then the polarization is no more circular but linear.
With the radial QAMC, the AR level of the $AS_{R\text{-}QAMC}$ is less than 3dB from 0.5GHz to 4GHz i.e. a relative bandwidth of 157%. But if we only considered the bandwidth in which the broadside RHCP gain of the $AS_{C\text{-}QAMC}$ and $AS_{R\text{-}QAMC}$ is higher than AS_{Ref}, then the relative bandwidth of the $AS_{C\text{-}QAMC}$ decreases to 67% and the relative bandwidth of the $AS_{R\text{-}QAMC}$ remains to 79% i.e. a difference of 12% between the two configurations.

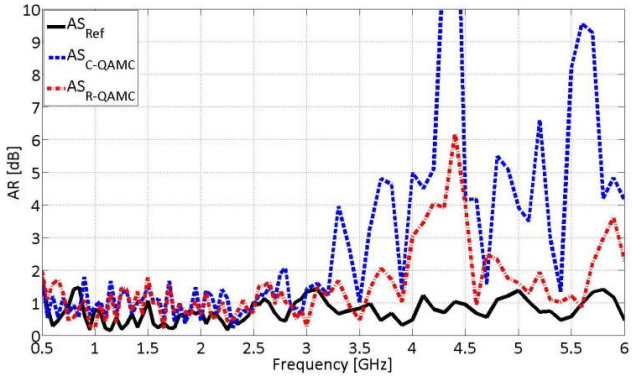

Figure 12: Axial ratio versus frequency.

Table 1 summarizes the measurements results. Those are given from 1.65GHz to 3.8GHz, which corresponds to the operational bandwidth of 79%.

Table 1: Radiation characteristics comparison between the two QAMC.

	$AS_{C\text{-}QAMC}$	$AS_{R\text{-}QAMC}$
Return Loss	< -10dB	< -10dB
Co-polarization Level (RHCP broadside gain)	3dB to 7dB	3dB to 9dB
Cross-polarization Level (LHCP broadside gain)	< -6dB	< -12dB
Axial Ratio	< 5dB	< 2dB

Finally, it is important to check if the radiation pattern is stable on the desired bandwidth. That means that the beam stays directional and the broadside RHCP gain does not present any sharp variations.
The following figures present the radiation patterns (in dB) for all configurations. All results are normalized by the value of the broadside RHCP gain.

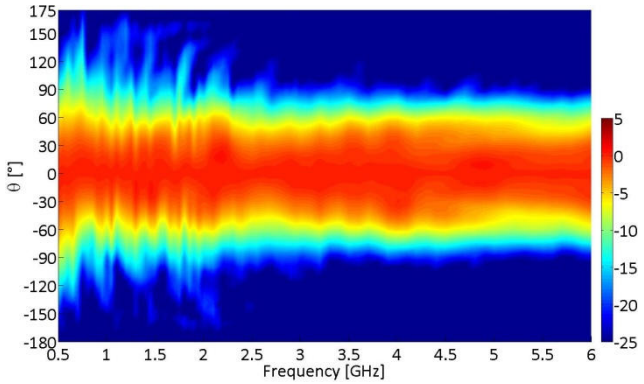

Figure 13: AS_{Ref} radiation pattern versus frequency for φ=0°.

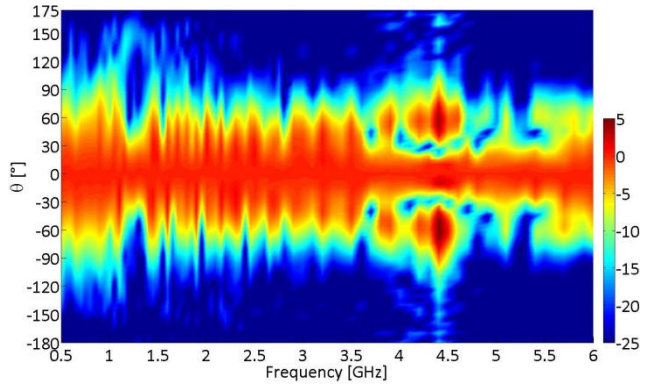

Figure 14: $AS_{C\text{-}QAMC}$ radiation pattern versus frequency for φ=0°.

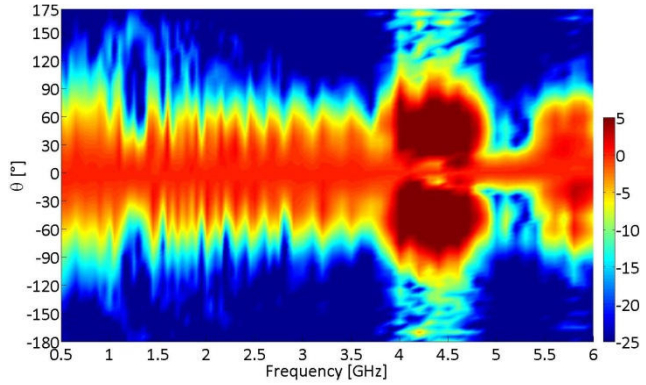

Figure 15: $AS_{R\text{-}QAMC}$ radiation pattern versus frequency for φ=0°.

The radiation pattern of the AS_{Ref} is stable from 0.5GHz to 6GHz, thanks to the absorber cavity (cf. Fig. 13).
Fig. 14 and 15 show that radiation patterns of the $AS_{C\text{-}QAMC}$ and the $AS_{R\text{-}QAMC}$ are almost similar from 0.5GHz to 3.6GHz. For frequencies higher than 3.6GHz the radiation pattern of the $AS_{C\text{-}QAMC}$ begins to be disturbed.
The radiation pattern of the $AS_{R\text{-}QAMC}$ stays stable up to 3.8GHz, and then it also begins to be disturbed, but in the center of the radial QAMC there is enough space to put another reflector in order to reduce this discontinuity.

6. Conclusions

We have shown that it is possible to design a radial QAMC reflector suitable to the geometry and the radiation of the Archimedean spiral antenna. The method consists in determining the active area and in designing circular patches with the dimensions given by the cartesian AMC. The simulation shows that the RHCP broadside gain of the two QAMC is almost similar.
In order to validate these results an Archimedean spiral antenna printed on Duroid RT 5880 substrate has been realized and placed 4mm above the two QAMC. Measurements results show a relative bandwidth of 79%, larger than the theoretical bandwidth of 66%, defined by a reflection phase included between +/-120°. With the radial QAMC the broadside LHCP gain is improved and the axial ratio is below 2dB from 1.65GHz to 3.8GHz.

The paper demonstrates that an Archimedean spiral antenna placed above a radial QAMC can achieve wideband properties with a thickness of only $\lambda_{1.65GHz}/15.3$. This new design can be improved by reducing the dimensions of the patches in order to have different patches for different frequency bands.

References

[1] D. Sievenpiper, L. Zhang, R. F. J. Broas, N. G. Alexopolous and E. Yablonovitch, High impedance electromagnetic surfaces with a forbidden frequency band, *IEEE Trans. on Microwave Theory and Techniques*, Vol. 47, No. 11, 2059–2074, 1999.

[2] M. Grelier, M. Jousset, S. Mallégol, A.C. Lepage, X. Begaud and J.M. Le Mener, Wideband QAMC reflector's antenna for low profile applications, *Applied Physics A: Materials Science & Processing*, Vol. 103, Num. 3, 809-813, 2010.

[3] J.A. Kaiser, The Archimedean two-wire spiral antenna, *IEE Trans. on Antennas and Propagation*, Vol. 8, No. 3, 312-323, 1960.

[4] Y. Mushiake, Self-complementary antennas, *Antennas and Propagation Magazine IEEE*, vol.34, no.6, pp.23-29, Dec 1992.

[5] F. Yang and Y. Rahmat-Samii, Reflection phase characterizations of the EBG ground plane for low profile wire antenna application, *IEEE Trans. on Antennas and Propagation*, Vol. 51, No. 10, 2691-2703, 2003.

[6] F. Linot, R. Cousin, X. Begaud, M. Soiron, Design and measurement of High Impedance Surface, *Antennas and Propagation (EuCAP), Proceedings of the Fourth European Conference on*, pp.1-4, 12-16 April 2010

[7] G. Goussetis, A.P. Feresidis, J.C. Vardaxoglou, Tailoring the AMC and EBG characteristics of periodic metallic arrays printed on grounded dielectric substrate, *Antennas and Propagation, IEEE Transactions on*, vol.54, no.1, pp. 82- 89, Jan. 2006.

[8] C. Djoma, X. Begaud, A.C. Lepage, S Mallégol and M. Jousset, Wideband Reflector for Archimedean Spiral Antenna, *6th European Conference on Antennas and Propagation 2012*.

[9] M. Grelier, M. Jousset, S. Mallégol and X. Begaud, *Antenna device with a planar antenna and a wide band reflector and method of realizing of the reflector*, Patent n° EP 2365584.

[10] M.N. Afsar, W. Yong, D. Hanyi, A new wideband cavity-backed spiral antenna, *Antennas and Propagation Society International Symposium*, vol.4, pp.124-127, 2001.